Moonen, P., Haagsman, H. P., Van Deenen, L. L. M., & Wirtz, K. W. A. (1979) *Eur. J. Biochem. 99*, 439–445.
Papahadjopoulos, D., Hui, S., Vail, W. J., & Poste, G. (1976) *Biochim. Biophys. Acta 448*, 245–264.
Peterson, G. L. (1977) *Anal. Biochem. 83*, 346–356.
Reynolds, J. A., Tanford, C., & Stone, W. L. (1977) *Proc. Natl. Acad. Sci. U.S.A. 74*, 3796–3799.
Roseman, M. A., & Thompson, T. E. (1980) *Biochemistry 19*, 439–444.
Ross, A. H., Radhakrishnan, R., Robson, R. J., & Khorana, H. G. (1982) *J. Biol. Chem. 257*, 4152–4161.
Segrest, J. P., Kahane, I., Jackson, R. L., & Marchesi, V. T. (1973) *Arch. Biochem. Biophys. 155*, 167–183.
Smith, R., & Tanford, C. (1972) *J. Mol. Biol. 67*, 75–83.
Smith, R. A. G., & Knowles, J. R. (1975) *J. Chem. Soc., Perkin Trans. 2*, 686–694.
Spiess, M., Brunner, J., & Semenza, G. (1982) *J. Biol. Chem. 257*, 2370–2377.
Steck, T. L., & Kant, J. A. (1974) *Methods Enzymol. 31*, 172–180.
Stoffel, W., Salm, K.-P., & Müller, M. (1982) *Hoppe-Seyler's Z. Physiol. Chem. 363*, 1–18.
Thenot, J.-P., Horning, E. C., Stafford, M., & Horning, M. G. (1972) *Anal. Lett. 5*, 217–223.
Van Zoelen, E. J. J., Twaal, R. F. A., Reuvers, F. A. M., Demel, R. A., & Van Deenen, L. L. M. (1977) *Biochim. Biophys. Acta 464*, 482–492.
Vaver, V. A., Ushakov, A. N., & Tsirenina, M. L. (1979) *Bioorg. Khim. 5*, 1520–1530.
Zilversmit, D. B., & Hughes, M. E. (1977) *Biochim. Biophys. Acta 469*, 99–110.

Structure and Kinetics of the Photoproduct of Carboxymyoglobin at Low Temperatures: An X-ray Absorption Study†

B. Chance,* R. Fischetti, and L. Powers

ABSTRACT: Photolysis and recombination of carboxymyoglobin at low temperatures have been studied by a variety of methods. This paper combines optical and structural studies of carboxymyoglobin photolysis and recombination in the temperature range 4–120 K. The absorbance changes indicate ablation of the characteristic optical transitions of carboxymyoglobin and formation of a photoproduct (Mb*CO) differing from deoxymyoglobin. When the X-ray absorption changes in the 7150–7200-eV region of the X-ray absorption spectrum are used as an indicator of structural change, the photoproduct at 4 K as measured with respect to the unphotolyzed sample is 60% of that observed for the chemically produced deoxy form. Saturation of the change is obtained with repetitive flashes totaling several thousand joules of energy from a xenon flash lamp by using a thin sample (1 mm) at 4 mM concentration as measured by both optical transmission and X-ray absorption criteria. The kinetics of the reaction show the change to occur at 10 K within the resolving time currently available (2 s) in the X-ray absorption measurements. The amplitude of the light-induced change decreases to half its maximal value at 40 K and to zero at 90 K. Steady illumination suggests at least two recombination processes. Analysis of the extended X-ray absorption fine structure (EXAFS) data on Mb*CO indicates small distance changes in the first shell of Fe–N and Fe–C that can be attributed to lengthening of the pyrrole nitrogen bonds and proximal histidine motion, together with a small displacement of the CO molecule on photolysis—a form here designated Mb*CO. This structure of the geminate state, Mb*CO, may elucidate the nature of elementary steps in chemical reactions and in tunneling processes.

In 1928, the wavelength-specific photolysis of iron carbonyls was used by Otto Warburg to identify "Atmungsferment" (Warburg, 1948; Bücher, 1947), later called cytochrome oxidase (Keilin, 1966). This ingeneous indirect method involved photolysis of the heme–CO compound in the presence of oxygen and was later perfected for a variety of oxidases including cytochrome *o* (Chance et al., 1953). Spectral observation of this photolysis was obtained at near freezing temperatures (Chance, 1953) and at lower temperatures (Chance et al., 1965). Curiously enough, the temperature dependence of recombination of CO and myoglobin could be observed at much lower temperatures than cytochrome oxidase as shown by Yonetani et al. (1973), who recorded the kinetics of the recombination reaction to 4.2 K (Iizuka et al., 1974). These kinetics were studied in detail by Frauenfelder and his colleagues (Austin et al., 1973, 1975; Alberding et al., 1976a,b, 1978; Alben et al., 1980), who emphasized the nonexponential nature of the reaction kinetics. While the optical method gave no clue as to the nature of the structural change that accompanies the flash-induced photolysis of carboxymyoglobin (MbCO), their results suggested that it would be best demonstrated at 4.2 K where the recombination rate is slow and the motion of the CO molecule away from the heme is limited.

The existence of an optical property of the photoproduct (Mb*CO) different from deoxymyoblobin (Mb) was supported by a shift of the absorption band of Mb*CO with respect to that of Mb by 14 nm, from 758 to 772 nm at 4.2 K (Iizuka et al., 1974). As the temperature increases toward 30 K, the

† From the Johnson Research Foundation, University of Pennsylvania School of Medicine, Philadelphia, Pennsylvania 19104 (B.C. and R.F.), and Bell Telephone Laboratories, Murray Hill, New Jersey 07974 (L.P.). *Received November 16, 1982; revised manuscript received March 22, 1983.* The portion of this research done at the University of Pennsylvania was supported by National Institutes of Health Grants GM-27308, HL-15061, GM-27476, and GM-28385 and National Science Foundation Grant PCM-80-26684. The work was done partially at the Stanford Synchrotron Radiation Laboratory (Project 632B and 660B), which is supported by the NSF through the Division of Materials Research and the NIH through the Biotechnology Resource Program in the Division of Research Resources in cooperation with the Department of Energy.

0006-2960/83/0422-3820$01.50/0

Mb*CO absorption band disappears due to recombination with CO. In the case of hemoglobin, an early photoproduct is that identified at room temperature as the "rapidly reacting form" of Gibson (1959), but this form is not observed in carboxymyoglobin photolysis at room temperature (Henry et al., 1983). Resonance Raman spectroscopy further indicates that the π-electron distribution and the stretching frequency of the FeN_ϵ (see Table I) in Mb*CO at 10 ns (at room temperature) is approximately the same as in deoxy-Mb (Friedman et al., 1982a,b). Thus low temperatures appear to be essential for the study of Mb*CO.

Alberding et al. (1976) found a very low activation energy of the recombination reaction and proposed a tunneling process. In order to evaluate ligand motions in such a proposed tunneling process, we have undertaken structural studies of Mb*CO.

A method affording measurement of structural changes of Mb*CO with respect to Mb and MbCO was required, and in 1979 the first data were obtained at 4 K by the extended X-ray absorption fine structure (EXAFS) method, which determines alterations in the distances of the first, second, and third shell ligands of iron porphyrins (Chance & Powers, 1981a,b; Fischetti et al., 1981), as first used in the study of hemoglobin (Eisenberger et al., 1978) and more recently of cytochrome oxidase (Powers et al., 1981, 1982; Chance & Powers, 1981a; Chance et al., 1980a). The findings have been consistent since the early observation, indicating small structural changes on photolysis and pointing, for the first time, to the possibility that the ligand remains close to the iron atom and that the $Fe-N_p$(pyrrole) distances lengthen characteristic of the change from MbCO to Mb is incomplete. Since the changes were found to be very small (<0.05 Å), special attention has been focused upon the achievement of experimental data of unusually high accuracy. The study employs states of MbCO, Mb*CO, and Mb that were as fully occupied as possible, either by the use of a chemically pure species or, in the case of Mb*CO, by exhaustive photolysis at the lowest temperature (4 K) feasible with the appropriate controls on optical and X-ray absorption changes. Last but not least, evaluation of the effect of X irradiation upon the samples was made both continuously and intermittently on-line and off-line by optical and electron paramagnetic resonance (EPR) criteria. We are able to describe structural features of the geminate state at 4 K, which we here identify as Mb*CO, which indicate retention of the ligand near the iron.

The alterations of electronic structure that occur in low temperature photolysis were studied by Spartalian et al. (1976) and later by Marcolin et al. (1979) at 4 K. Both noted significant differences between the photoproduct and Mb, and the latter identified the photoproduct to be a ferrous high-spin complex with Mössbauer parameters differing from that of Mb. The latter proposed that "the difference in electronic structure might be caused by the nearby CO molecule: in Mb*, the CO molecule remains in the heme pocket after photodissociation and has measurable influence over the electronic structure of the heme iron whereas in the case of Mb, the CO is removed from the heme pocket." This interpretation agrees with the perturbation of the 758-nm band of Mb to 772 nm in Mb*CO and to the infrared data of Alben et al. (1980), who proposed "incomplete relaxation of the iron atom in Mb*" (Alben et al., 1982).[1]

Cornelius et al. (1981), using fast time resolved studies, found that the half-time for the formation of Mb*CO is <6 ps at 23 °C. The intermediate is stable from 40 ps to 10 ns. The difference spectra from the work of Iizuka et al. (1974) at helium temperatures correspond to those of Cornelius et al. (1981) at 273 K, the isosbestic point being at 431 nm and the peak of the difference spectrum being 440 nm in both cases, distinctly different from that of Mb. Recent work by Eaton and his co-workers (Henry et al., 1983) shows the deoxy state rather than Mb*CO to predominate from 3 ns onward. It is noteworthy that Hasinoff (1981) finds, at >180 K, that the quantum yield changes with flashes of increasing duration, suggesting that photolysis and recombination occur repeatedly, resulting in the accumulation of Mb rather than Mb*CO.

Glycerol glasses have been frequently used in optical studies (70% glycerol; Austin et al., 1973). Recombination reactions at higher temperatures have been reported by Hasinoff (1981), who found that the apparent energies of activation depend upon whether glycerol or ethylene glycol was used. In this study, we have been able to use either frozen buffer or a 30% mixture of ethylene glycol, which has been shown to cause no detectable difference in the kinetics of the reactions with MbCO or with the more delicate membrane protein cytochrome oxidase (Powers et al., 1981; Chance et al., 1975; unpublished observations).

Materials and Methods

General descriptions of the systems used for X-ray absorption measurements are given by Powers et al. (1981) and by Chance et al. (1982a–c) for the methods of sample preparations. Here we describe the cryostat for the low-temperature studies.

Cryogenic Techniques. The Air Products Helitran No. LT-3-110 was employed in order to achieve temperature-stabilized states of carboxymyoglobin between 4 and 200 K. Furthermore, an adequate solid angle of X-ray viewing (6% of 4π) was obtained with the heat shield in place, and adequate transmission and emission of X-rays was obtained by installing 5–10-mil mylar windows. The elliptical sample holder (4 × 11 mm) was made of copper and was screwed into the cold finger. The thickness of the sample was limited to 1 mm to facilitate photolysis. Two sample holders were fitted into the cold finger, a reference sample and a sample that was to be illuminated by visible light and by X-rays [see Figure 1 of Chance et al. (1982a)]. The sample holder was turned at 45° with respect to the excitation X-ray beam; a manganese oxide filter was mounted on the heat-shield aperature and was used to enhance the ratio of Fe Kα fluorescence photons to elastically scattered excitation photons that are counted by a Pilot B plastic-coated scintillation counter (Powers et al., 1981; Chance et al., 1982a). The backside of the sample was illuminated by visible light in the region of 500–700 nm, and the spectrophotometer afforded reflectance spectroscopy of the extent of photolysis and possible sample damage (Chance et al., 1980b). Transmission spectroscopy of the sample in the 700–800-nm region was also employed.

Flash photolysis of the sample was achieved by remote control of a flash lamp that was lowered in front of the cryostat to intercept the X-ray beam and to afford flash illumination of the front face of the sample of 200 J/flash. The lamp was then immediately raised, allowing the X-ray beam to reilluminate the sample. The whole maneuver required 2 s and was accomplished by a string and pulley arrangement accessible to the outside of the hutch.

A drawing of the apparatus is afforded by Figure 1, which illustrates the path of the incident X-ray beam to the sample and shows the scintillation detector at a 90° angle to the beam; the helium evaporator is within the vacuum shroud to which

[1] Here Mb* is used to designate photoproduct and is the same state we designate as Mb*CO.

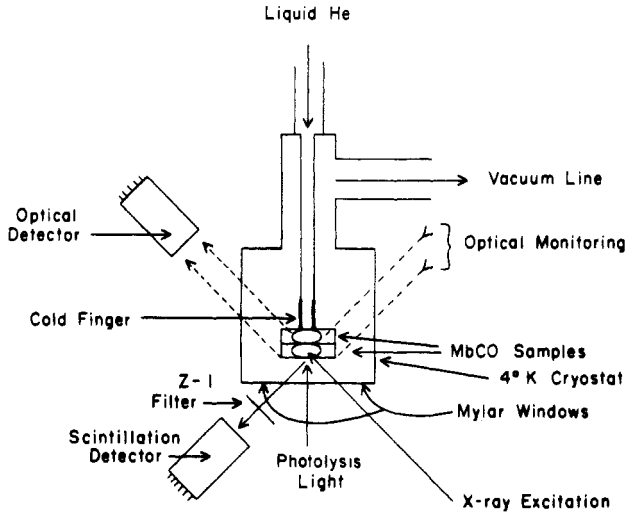

FIGURE 1: Experimental setup for determining optical and EXAFS data from illuminated and nonilluminated MbCO in the temperature region of 4 K. The line labeled X-ray excitation is in the direction of the X-ray beam; the fluorescence photons are collected at a right angle by the scintillation detector. The sample is maintained at low temperatures by the helium evaporator, appropriately evacuated by the vacuum line. The backside of the sample is illuminated by a tunsten lamp, and reflectance spectra are obtained by electron multiplier detectors.

the vacuum line is attached. Optical measurements may be afforded by illuminating the backside of the sample with a tungsten filament lamp, and photodetection is by silicon diode detectors with appropriate filters. This version of the sample employs an end-on photomultiplier and 30-Hz time-shared monochromatic illumination of a reference and measured sample (Chance et al., 1982a).

Monitoring of Sample Damage. The backside of the sample is continuously monitored during the EXAFS experiment, not only for the degree of photolysis as indicated above but also for X-ray damage of the sample. Hydrated electrons, observed to be damaging to the redox state of the sample in studies of oxidized cytochrome oxidase at temperatures above 173 K (Chance et al., 1980b; Powers et al., 1981), do not appear to have an effect upon the already reduced MbCO, especially at the very low temperatures employed here. More recent data indicate the reduction rate at −130 K is $\leq 2.5 \times 10^{-3}$ μM/s (L. Powers and B. Chance, unpublished observations). However, the optical properties of the sample may vary due to condensation of gases on the face of the sample used for optical studies, causing the intensity of the absorption, for example, at 540 and 560 nm, to decrease significantly with a half-time of 2 h. The absorbance decreases exponentially, but to a plateau value that allows us to distinguish this effect from an irreversible effect of the X-rays. In addition, warming and cleaning the sample surface restores the signal diminished by condensation. These effects seem negligible at 700–800 nm. If, however, an irreversible change is observed that exceeds 10% of the absorption spectrum at these wavelengths, the sample is replaced.

Sample Heating. The possibility of heating the sample (200-J incident on the sample) is tested by a quickly responding thermocouple in the sample volume or from a carbon resistor the same size as the sample; these indicate a thermal transition of 1 s during which the temperature may rise several degrees above 10 K, the temperature at which the test was made. In this case, the radiation above 650 nm was diminished by a Corning 9782 filter. Thus, the possibility that the temperature of the sample is raised to a value at which some recombination can occur is minor in the case of MbCO, which recombines very slowly even at 20 K, but could be significant with the reactions of other pigments such as hemoglobin, where rapid recombination can occur prior to thermal reequilibration of the sample and the Cu block in which it is contained.

Degassing under Cryogenic Conditions. The sample is in an evacuated space under the conditions of observation, and loss of carbon monoxide from the sample is undesirable. While this is apparently quite slow at 10 K, problems may arise on changing samples. In order to insert a fresh sample on the cryostat, it is necessary to warm the cold finger to a manageable temperature such as 100–150 K. The cold finger is then removed from the shroud of the cryostat, the heat shield is removed, and the existing samples are removed from the spring clips that retain them. The fresh sample previously maintained at liquid nitrogen temperatures is then inserted by hand, the heat shield is reinstalled, and the cold finger is reinserted into the shroud. Under these conditions, the temperature may rise as high as 200 K. The application of vacuum immediately to the exposed sample may result in rapid degassing and disruption of the surface of the sample by bubble formation, particularly when the sample contains 30% ethylene glycol. In nearly all cases, this problem is minimized by employing a sample chamber that has mylar walls.

Sample Chamber. A mylar-covered sample chamber is formed by applying mylar tape to both sides of an elliptical hole in a copper block and filling the sample through a needle hole in the bottom. The gas effluxes through the corresponding exit hole at the top. When the redox titrator (Chance et al., 1982c) is employed, then the sample is automatically filled by direct connection to the redox-equilibrated volume.

Sample Preparations. Horse or sperm whale myoglobin (Sigma, 95–100%) is weighed out to a concentration between 4 and 10 mM and dissolved in a 15 or 30% solution of ethylene glycol in 50 mM phosphate buffer (pH 7.0). The sample is centrifuged to remove insoluble material. The purity is determined by optical examination of aliquots (>95%). The solution is saturated with CO, a slight molar excess of dithionite is added, and the sample is immediately inserted into the sample chamber by a syringe connection and is frozen in liquid nitrogen in a time of ~2 min. Some 30% ethylene glycol is added to avoid formation of eutectics and microcrystalline regions that give energy-dependent X-ray scattering.

Samples are also prepared by incubating myoglobin in a redox equilibration chamber where the redox potential is monitored by a platinum/calomel electrode and exposure to oxygen is eliminated by a continuous flow of carbon monoxide (Chance et al., 1982c). Such preparations assume a potential of −200 mV with partial or nearly complete reduction of the myoglobin and conversion to the MbCO compound. However, in order to eliminate any possibility of the presence of metmyoglobin, the potential is diminished to −450 mV by titration with dithionite solution prepared in CO-saturated buffer. A stainless-steel transfer tube that has first been purged of oxygen by continuous flow of CO is plunged below the surface of the MbCO in order to initiate the transfer. The pressure on the titrator is sufficient to transfer the sample through the drill hole of the above-mentioned mylar-walled sample holder. As described above, such samples are free of metmyoglobin and show complete photolysis as assayed by reflectance spectroscopy.

Criteria for Sample Alteration. The samples were assayed prior to and following flash photolysis in the helium cryostat; in short, three parameters were assayed: (A) maintenance of MbCO concentration in the dark; (B) completeness of MbCO

photolysis on flash illumination; and (C) radiation damage. Should any of these parameters deviate by 10%, the sample was replaced.

Photolysis of Various Concentrations of MbCO. In a variety of publications, photolysis of both dilute and concentrated samples of iron carbonyl compounds has been studied without experimental studies on the extent of photolysis, particularly those using Mössbauer techniques requiring dense samples (Marcolin et al., 1979; Spartalian et al., 1976).

Some obvious criteria of the spectra presented below determine the efficiency of the photolysis reaction; the first of these is that incomplete photolysis should be indicated by the remnant absorption of MbCO in transmission spectroscopy or, as mentioned below, backside reflectance spectroscopy. The optical data further indicate the formation of an anomalous reaction product at 4 K, Mb*CO, absorbing at 772 nm in accordance with Iizuka et al. (1974).

On the basis of our previous experience with thin samples (Chance, 1953), we have recognized the problem of the thick samples and have employed the following procedures: (1) xenon flash illumination for activation of photolysis (350 to >1000 nm) was used and has been compared with monochromatic light; (2) repetitive flashes were spaced at intervals of 1 s or greater, which would avoid accumulative sample heating and permit spectroscopic recording between flash intervals; (3) reflectance spectroscopy of the α bands of MbCO has been obtained from the opposite side of the sample from that flash photolyzed; (4) transmission spectroscopy of the near-infrared absorption band of Mb has been obtained following a series of flashes; (5) a series of optical filters have been used to evaluate the action spectrum for xenon flash photolysis of carboxymyoglobin at 4 K; and (6) X-ray absorption spectroscopic evaluation was used. Only the most relevant of the above controls are displayed in the following figures.

Backside Reflectance Spectroscopy. Figure 2A shows reflectance spectra of a concentrated MbCO sample as measured by reflectance spectroscopy from the opposite's face to that illuminated in response to increasing numbers of incident xenon flashes. The illumination was obtained from a coiled GE flash lamp (type No. FT 218) held within 5 mm of the mylar window of the helitran (~1 cm from the sample), operated at a power input of 200 J and flashed repetitively at one flash/s. Under the conditions of flashing, the sample is rotated so as to be perpendicular to the incident light. It is estimated that the efficiency of energy transfer under these conditions exceeds 10% and may be as high as 30%. Sample heating under these conditions, while significant during the flash, is insignificant on an accumulative basis (see below).

The disappearance of the characteristic 579- and 540-nm bands of MbCO indicates that these characteristic electronic transitions are ablated by the successive flashes at the low temperature. The absorption bands of the CO form at low temperature agree with those obtained under similar conditions by Iizuka et al. (1974). If one takes the elimination of the trough between the two peaks as a criteria of completion of photolysis, the effect is approximately 50% complete with eight flashes and over 90% complete with 16 flashes, which corresponds to 3200 J incident upon a 10 mM sample of 1-mm thickness. Since there is the possibility—remote in our case—that a portion of the flash intensity may have been reflected to the backside of the sample to cause photolysis, we have employed transmission measurements of 10 mM MbCO in a 1-mm thickness and, in order to achieve adequate signal to noise ratio, have employed the near-infrared absorption of

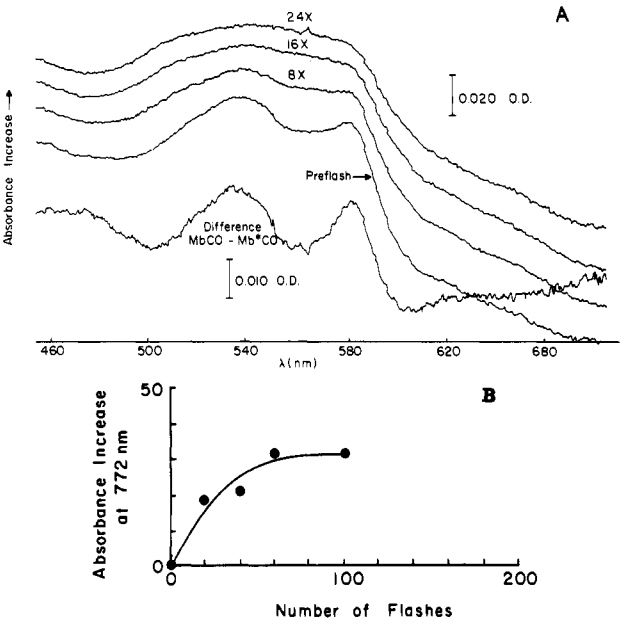

FIGURE 2: (A) Wavelength scans of MbCO at 4 K obtained by reflectance from the backside of the sample; the preflash spectrum identifies the two peaks of MbCO at 8, 16, and 24 times the incident flashes with the xenon flash lamp described in the text. The difference spectrum obtained at 2 times sensitivity is indicated in the bottom. (B) Illustration of effect of repetitive flashes upon increased absorbance of Mb*CO at 772 nm at 4–10 K using 10 mM Mb.

the Mb*CO at 772 nm (Iizuka et al., 1974). Half-maximal effect is obtained with <20 flashes, and saturation (>90%) occurs at an estimated 50 flashes (10^4 J). These are values that are higher than those obtained by backside reflectance, and these integrated intensities have been used in experiments below, which are employed for structural analysis. In the case of kinetic studies, where the time response and not the extent of response was important, we have used a smaller number of flashes. In fact, when indicator energies and front-face reflectance are used, adequate X-ray absorption signals are obtained with 0.10 the number of flashes used for structural studies.

Since the calculated absorbance from monochromatic light at the major absorption bands is very high, we have explored the question of the efficiency of the white light in the near-infrared region. We found it not possible to reproduce the results obtained with white light using comparable energies (as estimated from the energy distribution of the white light) by using the monochromatic light of a liquid dye laser and have concluded that "hole burning" in the trapped states makes monochromatic light ineffective in determining the 4 K action spectrum. In order to ensure accurate transmission spectrophotometry, we have used transmission measurements at 772 nm of 0.2 mM MbCO (see below for justification of this concentration) in the same sample geometry as used above. The results are displayed in Figure 3. We have progressively diminished the blue-light content of the xenon flash lamp by using a succession of Wratten filters 2b, 4, 16, 24, and 29, giving, respectively, 50% transmission at 390, 470, 540, 595, and 620 nm. These Wratten filters have been tested in detail to ensure that they do not to have significant transmission in their cut-off region (in a number of cases the attenuation is at least 10^4 and generally 10^6; D. Meyer, personal communication).

Taking, for example, light above 540 nm as a reference filter, it is seen that the filter passing light above 595 nm is only 3 times less efficient, while the filter passing light above

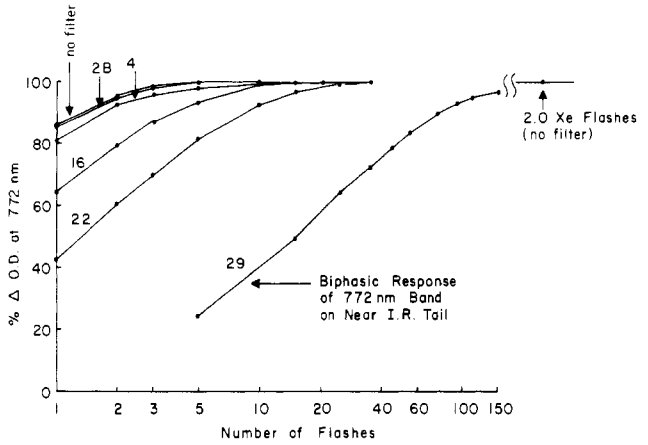

FIGURE 3: Flash response of 0.2 M MbCO as a function of illumination wavelength at 4.2 K. The numbers indicate the Wratten filter used on the xenon flash.

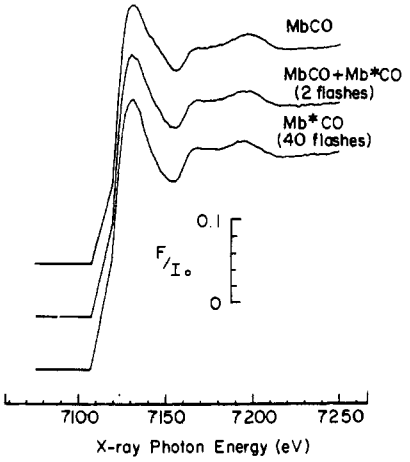

FIGURE 4: Short X-ray absorption scans of indicator energy region for MbCO (top), after two flashes (middle), and after 40 flashes, giving Mb*CO (bottom). A linear background has been subtracted to set the absorption below the edge equal to zero. Data were collected by fluorescence, F, and I_0 is the incident intensity.

620 nm, in a region where no strong transitions in the absorption spectrum of the carboxy species are recognized, has decreased the efficiency 20-fold. The choice of 0.2 mM MbCO was dictated on the basis of experimental feasibility; not only is it difficult to obtain transmission spectra through the more concentrated samples, as in Figure 2B, but also the number of xenon flashes required for 90% effect with the Wratten 29 filter becomes very large. Nevertheless, we presume that the decrease of efficiency between 540 and 620 nm would be even less at 10 than at 0.2 mM.

A consequence of these studies is that the optical depth for xenon flash activation of the front face approximates the X-ray depth to an extent that would be expected on the basis of their absorption coefficients at 7 keV and >600 nm, respectively. For example, Figure 4 shows about 85% of the X-ray absorbance change is obtained with two flashes. Thus front-face reflectance and X-ray absorption spectroscopy may be in apparent agreement. In the experiments cited below where structural factors are determined, we have employed 40 or more flashes as indicated by Figure 2B. On the other hand, one or two flashes give an acceptable change in the X-ray absorption signal for the kinetic studies.

X-ray Absorption Measurements and Data Analysis. Data were recorded at the Stanford Synchrotron Radiation Laboratory under dedicated operating conditions of the SPEAR storage ring on beam line II-3. The focusing mirror was raised

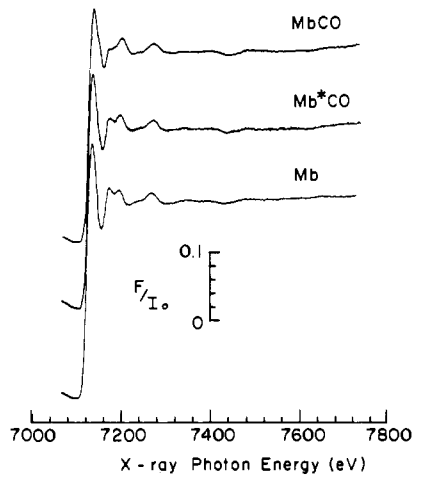

FIGURE 5: X-ray absorption spectra of MbCO (top), Mb*CO (middle), and Mb (bottom).

to a position sufficient to give 2–3-eV resolution with Si 111 monochromator crystals. Under these conditions, $\sim 10^{10}$ photons/s were delivered to the sample in a focal spot size of ~ 2 mm × 4 mm to ~ 5 mm × 8 mm, depending on the condition of the beam-line components.

The X-ray absorption data were analyzed by procedures discussed previously (Powers et al., 1979, 1981, 1982; Lee et al., 1981; Peisach et al., 1982). Short scans (Figure 4) covering a 7050–7250-eV energy range were collected in 4 min each by measuring two points below the edge (2 s each), 17 points over the edge maximum (1 s each), and 59 points (4 s each) in the energy range above the edge. These were analyzed in a manner similar to that of edge data (Powers et al., 1979, 1981) where the absorption below the edge is set to zero by subtraction of a straight-line background. Measurements of intensity changes in the oscillations above the edge were compared to each other by a tangent line drawn to the first minimum at 7150 eV and the flat region between 7200 and 7250 eV. Normalization of these changes by the edge jump was not necessary as all kinetic data were taken in the same storage ring fill under identical conditions. Comparisons with deoxy or met states required normalization, as they were measured in different fills of the storage ring but under the same conditions.

Longer scans covering the entire EXAFS region were obtained at 2 s/point (Figure 5). These were analyzed by methods discussed previously (Powers et al., 1981; Lee et al., 1981; Peisach et al., 1982), including background substraction and k^3 (wave vector) multiplication (Figure 6) followed by Fourier transformation (Figure 7). [k^2 multiplication was also used to enhance the differences observed at low k and yields the same results.] The isolated first-shell contributions (filtered data, Figure 8) were fit to Fe–N contributions by using the model compound bis(imidazole)($\alpha,\beta,\gamma,\Delta$-tetraphenylporphinato)iron(III) chloride (Im_2FeTPP) having 6 N at 1.986 Å (Collins et al., 1972) and to a Fe–C contribution by using both $K_3Fe(CN)_6$ with 6 C at 1.903 Å (Figgis et al., 1969) and $Na_2Fe(CO)_4$ having 4 C at 1.746 Å (Teller et al., 1977; Chin & Bau, 1976). Each contribution in the fitting procedure is represented by an average distance, r, an amplitude factor containing the number of ligands, a change in the Debye–Waller factor with respect to the model compound, $\Delta\sigma^2$, and a change in threshold with respect to the model. Although the latter was always small (≤3 eV), the amplitude factor and change in Debye–Waller contribution are generally highly correlated and precautions were taken to avoid pitfalls

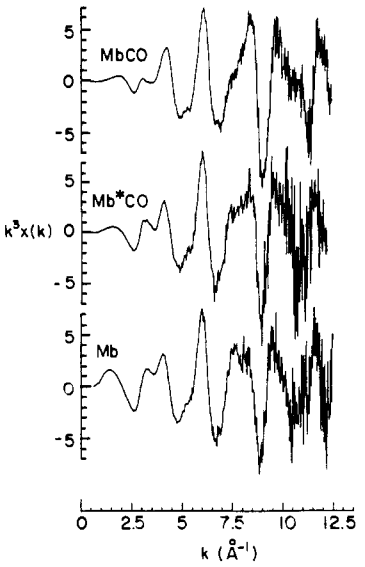

FIGURE 6: Background-subtracted EXAFS data after k^3 multiplication and normalization to one iron atom for MbCO (top), Mb*CO (middle), and Mb (bottom).

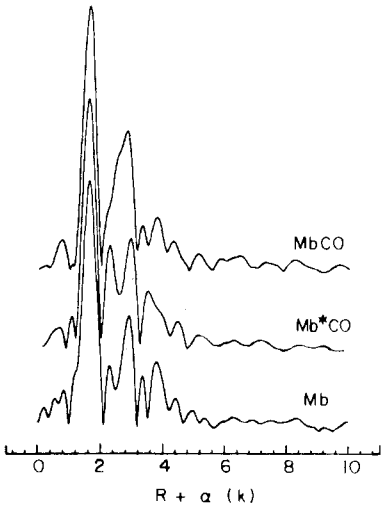

FIGURE 7: Fourier transformation of EXAFS data of Figure 4 for MbCO (top), Mb*CO (middle), and Mb (bottom). $\alpha(k)$ is the absorber–scatterer phase shift (Powers et al., 1981).

yielding erroneous results that have been described in detail by Peisach et al. (1982). The amplitude factors were therefore constrained to their known values, and little change was observed in the fitting parameters or the sum of the residuals squared, $\sum R^2$, when these were then allowed to vary. Although different Fe–C models were used for comparison of chemical environment (Eisenberger & Lengler, 1980), both gave identical average distances and comparable sums of residuals squared with small differences in the change in Debye–Waller contribution.

Results

The goal of one set of experiments was to determine the kinetics and extent of changes caused by low-temperature photolysis of the concentrated samples. The largest changes in the X-ray absorption spectra are observed at an "indicator energy" in the 7150–7200-eV region (Figure 4). The oscillations observed in this region of multiple scattering ($k \leq 4$ Å^{-1}; Azaroff, 1963; Stern, 1974; Belli et al., 1980) are due largely to contributions from the partially resolved second- and third-shell scatterers in the heme with a small contribution from the first-shell scatters. The changes observed are associated with lengthening of the Fe–N_p bonds and have therefore been useful to identify the extent and rate of the structural change on photolysis. The changes of the indicator energy complement the optical data described above since these changes are observed in the immediate environment of the iron atom while those obtained by reflectance spectroscopy reflect those of the electron cloud of the entire heme. In addition, inferences on the extent of photolysis and the rate were obtained by reflectance spectroscopy on the opposite side from the X-ray measurements.

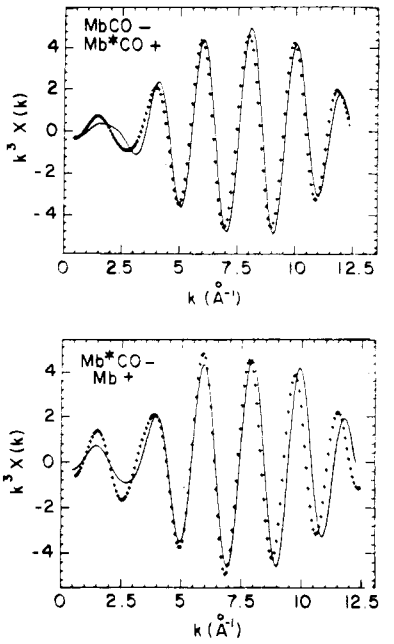

FIGURE 8: Comparison of first shell filtered data of MbCO (–) with Mb*CO (+) (top) and Mb*CO (–) with Mb (+) (bottom).

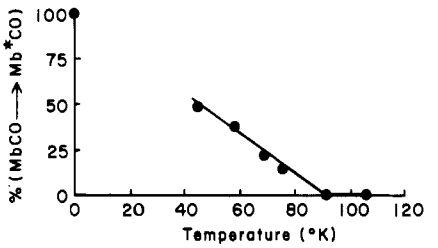

FIGURE 9: Effect of temperature on amplitude at the indicator energy of 7173 eV, suggesting that recombination is largely complete above 90 K.

Quantitation of the extent of photolysis and of other kinetic parameters is measured by the short-scan method (Figure 4). A value of 1.3 is found for the ratio of Mb*CO to MbCO in the indicator energy region, and the same comparison for Mb and MbCO gives 1.5. Thus, Mb*CO gives a change equal to 87 ± 5% of that for the Mb, measured with respect to MbCO. In tests with 40–80 flashes of the xenon flash lamp, this percentage does not appear to increase further. The change that corresponds to Mb*CO is always less than that corresponding to Mb.

Effect of Temperature on Extent of Photolysis. Recording in repetitive short scans of 4-min duration, we have measured the fractional change of the indicator energy of a sample flash photolyzed at 40 K as the temperature was allowed to rise slowly from 40 to 100 K over an interval of over 1 h. The decrease of the indicator energy was followed as a function of time and temperature (Figure 9). This profile indicates a linear decrease of the amplitude of change at the indicator energy, reaching 0 at about 90 K. No data were obtained from

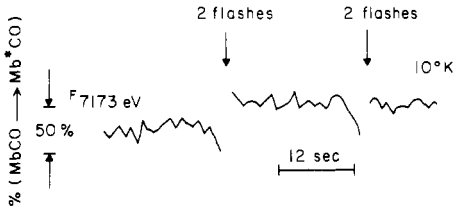

FIGURE 10: Kinetics of light-induced indicator energy change as a function of time (2 s/point, increasing from left to right) at 10 K, showing the effect of pairs of flashes on the amplitude at 7173 eV.

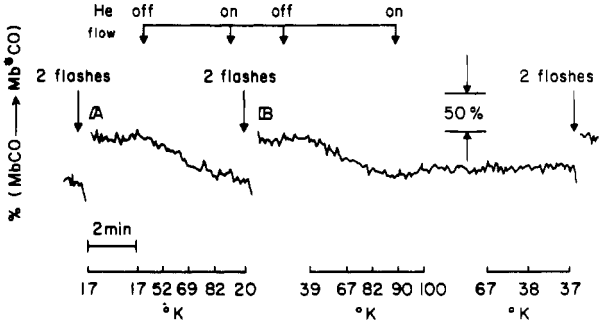

FIGURE 11: Effect of time and temperature upon indicator energy at 7173 eV for MbCO in the temperature region from 10 to 100 K (4 s/point).

4 to 40 K. These data are useful in identifying the fractional extent of change of the indicator energy at various temperatures as measured by repetitive scans (4-min duration), and the consistency of the data is demonstrated by the extrapolation.

Kinetics at the Indicator Energy. The time resolution in these measurements can be increased to 2 s/point, and the kinetics after the flash are shown in Figure 10. The particular sample of MbCO had previously been flash photolyzed at 10 K, warmed to 122 K, and then cooled to 10 K. The recording starts at the left-hand portion of the trace. The break of the trace is occasioned by intercepting the X-ray beam with the flash unit and twice flashing the sample, which requires 2 s. The first data point following the flash is displaced upward. The flash is then repeated, indicated by the second gap in the data. Thereupon, the further displacement of the trace is small. Thus, the structural change at 7173 eV occurs within the resolving time of the instrument and is relatively stable at 10 K. Any geminate recombination process would have to occur with a half-time less than 2 s at 10 K to be overlooked by this method, and none is found in the 8-ms–8-s interval (B. Chance et al., unpublished observations).

Temperature Perturbation with Continuous Recording at the Indicator Energy. A similar study can be made by recording continuously at the indicator energy where, in this case, data are plotted as a function of time, and the various temperatures are noted on the curves (4 s/point). The X-ray beam is obscured by the flash lamp during the flashes and then the beam is again allowed to impinge upon the sample. The upward deflection corresponds to the difference between Mb*CO and MbCO at the indicator energy (Figure 11, part A). Thereafter, the temperature remains at 17 K for approximately 2 min, and no measurable recombination of the sample is observed. At this point, a slow temperature jump is imposed upon the sample; the helium flow is throttled and the temperature rises to 69 K, and the helium flow is resumed. The temperature overshoots to 80 K and then falls rapidly to 20 K. During this interval, the change at 7173 eV has decreased very nearly to the base line. A second set of flashes in Figure 11, part B, gives a similar deflection, and again, in this case, the helium flow is throttled as earlier, and the temperature reaches 82 K in 3 min thereafter and is maintained at 90 K. The cooling occurs at the point marked with the arrow, yet at a slower rate due to lower helium flow. As the temperature falls to 37 K, a third flash gives a smaller deflection as expected from Figure 9. The temperature at which complete recombination occurs appears to be about 82 K, which is in reasonable agreement with the data of Figure 9, and these data furthermore clearly show the reversibility of the photoinduced structural change.

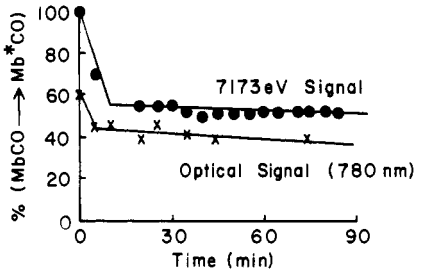

FIGURE 12: Slow temperature jump, 4–44 K in 5 min. The chart shows responses of indicator energy and optical signals as functions of time.

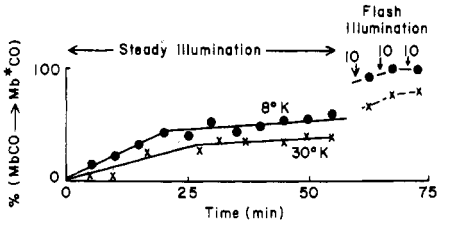

FIGURE 13: Comparison of effects of steady illumination (50-W tungsten lamp) upon rate and extent of change at indictor energy (7173 eV). The steady illumination is followed by intervals (10 each) of xenon flashes.

Slow Temperature Jump. Perturbation of the system containing predominantly Mb*CO to a new equilibrium state in the dark is indicated in Figure 12. Diminishing the helium flow to the cryotip and setting the heater at maximum, and resetting the helium flow and the heater at 44 K, gives a "5-min" jump. The response of the amplitude at the indicator energy is recorded every 3 min. At this temperature, about 50% recombination has occurred, presumably involving the geminate species. (While a more rapid temperature transient could be obtained by breaking the vacuum, we have found it difficult to avoid artifacts.)

Effect of Steady Illumination. Illumination with a 50-W tungsten lamp impinging directly upon the same side of the sample as illuminated by X-rays causes photolysis as measured at the indicator energy of 7173 eV (Figure 13). The increase with time of the indicator signal at 8 and 30 K gives different initial slopes and extents of reaction at the two temperatures and indicates a 2-fold greater rate of recombination at higher temperatures. Incomplete photolysis is observed at both temperatures as indicated by the further responses obtained with the xenon flash lamp, strongly supporting the use of the flash over steady illumination. The break in the slope at 20–25 min at the two temperatures indicates at least two rates of recombination.

Discussion

*EXAFS Data Analysis: Structure Differences in the Iron Site of MbCO and Mb*CO.* The first-shell filtered data of the MbCO and Mb*CO are shown in Figure 8. The amplitudes are comparable, with Mb*CO having only a slightly longer average distance, indicating that the CO ligand is not

Table I: Results of Two Contribution Fits Having Amplitude Factors Constrained to Known Values[a]

	MbCO				Mb*CO			
model compound (ligand)	r	N	$\Delta\sigma^2 \times 10^3$	ΣR^2	r	N	$\Delta\sigma^2 \times 10^3$	ΣR^2
Im_2FeTPP	2.01	4	2.6	2.0	2.03	4	3.8	0.54
Im_2FeTPP	2.17	2	2.0		2.19	2	3.3	
Im_2FeTPP	2.02	5	2.0	1.7	2.05	5	2.7	0.61
Im_2FeTPP	2.20	1	4.1		2.22	1	4.1	
ImFeTPP	2.05	5	0.5	2.5	2.07	5	−0.6	2.2
$Na_2Fe(CO)_4$ (or $K_3Fe(CN)_6$)	1.93	1	2.1		1.97	1	2.9	

[a] r is average distance ±0.02 Å. N is coordination number (constrained). $\Delta\sigma^2$ is change in Debye-Waller contribution with respect to the model compound in Å^2. ΣR^2 is sum of the residuals squared, indicating the quality of the fit.

lost in the first shell on photolysis. If only the CO ligand has moved, subtraction of these two filtered data removes the heme and proximal nitrogen contributions leaving the difference in the CO contributions. This difference was then fit with a two-contribution fit of Fe–C models, but the results were unphysical and had a very large sum of the residuals squared. This meant that changes also occurred in the heme and/or proximal nitrogen on photolysis or that Mb*CO was a mixture of states having different Fe–C(O) distances. Although the latter was unlikely from optical and indicator energy data (see above and Figure 2), reproduction of the filtered data of Mb*CO was attempted by a sum of the data for MbCO and Mb. The sum of residuals squared for the sum was nearly a factor of 15 larger than the constrained fits discussed below. This argument is further supported by the analysis of the data from an incompletely photolyzed sample that was exposed to only three flashes at 10 K. The EXAFS data were fitted optimally by a sum of 0.30 MbCO and 0.70 Mb*CO, respectively. The sum of the residuals squared was very low, 1.8. The indicator energy showed values of 0.20 and 0.80 for the two components, in reasonably good agreement with the EXAFS data analysis. Thus, the X-ray data analysis is capable of detecting incomplete photolysis when less than saturating flash intensities are used and of indicating complete photolysis when multiple flashes are used.

In the data analysis of the completely photolyzed samples, there may be three unresolved contributions to the first shell of each state [heme (Fe–N_p), proximal nitrogen (Fe–N_ϵ), and CO], all of which may change on photolysis. Three contributions to the single shell filtered data fitting procedure require more independent parameters than the number of degrees of freedom in the data and can therefore yield erroneous results (Lee et al., 1981; Peisach et al., 1982). Two contribution fits having the amplitude factors constrained to known values were therefore used, and the results are shown in Table I. The 4/2 ligand combination gives the average Fe–N_p distance and the average Fe–axial ligand distance. This average is a $1/r^2$ weighted average, and the larger the difference in the individual axial ligand distances, the larger the average distance deviates from an arithmetic average. For this reason, the 5/1 ligand fits attempt to determine the longer axial contribution (Fe–N_ϵ) separately with the shorter contribution (CO) averaged with the Fe–N_p contributions and vice versa.

Even though changes are small, CO displacement from Fe by 0.05 ± 0.03 Å on photolysis is accompanied by a lengthening of the Fe–N_p distance of the heme and possibly lengthening of the proximal nitrogen distance. Although these changes lie within the absolute error of the fitting procedures, the case of no change has been ruled out by the subtraction procedure discussed above. Lengthening of the pyrrole nitrogen distance is also supported by the shift of the absorption edge of 2 eV to lower energy on photolysis. Similar shifts are observed in model compounds and other heme proteins where this expansion is known regardless of the chemical type of axial ligands (Powers et al., 1982; Korszun & Moffit, 1982; Labhardt & Yuen, 1972). In addition, the fitting procedures for the chemical deoxy state yield an average Fe–N_p distance of 2.06 ± 0.02 Å with Fe–N_ϵ distance of 2.12 ± 0.02 Å in agreement with Takano (1977). Again, the absolute errors overlap for the Fe–N_p expansion of the Mb*CO and the Mb, but subtraction of the two does not give a single CO contribution. We therefore conclude that the Fe–N_p expansion of the photoproduct is not as large as Mb. Since the X-ray absorption technique only directly measures Fe–ligand distances, motion of the Fe with respect to the heme plane cannot be calculated without assumptions (Eisenberger et al., 1978; Perutz et al., 1982) and is not addressed here.

Comparison of the Fourier-transformed data (Figure 7) with that of Fe^{2+}PocPivP(1-MeIm)(CO), the Collman "pocket" model compound (Sessler, 1982), shows similarity in both the first and higher coordination shells, suggesting that the two pockets may be of similar structure.

Adequacy of Photolysis. The first and most important feature of photolysis of carboxymyglobin at low temperatures is that the product is not the deoxy form; the near-infrared spectrum shows a red shift of the deoxy form of approximately 15–772 nm, corresponding to an anomalous photoproduct Mb*CO, in agreement with the work of Iizuka et al. (1974) and consistent with observations by Mössbauer spectroscopy (Spartalian et al., 1976; Marcolin et al., 1979). However, this photoproduct appears not to be detectable by infrared absorption spectroscopy (Alben et al., 1982). The maximization of the concentration of a unique photoproduct does not in itself verify that all of the carboxy compound has been converted by the light reaction. For this reason, we have ensured that repeated flashing not only maximizes the infrared response as measured by transmission through the sample but also causes an ablation of detectable absorption due to the CO compound. The particular conditions for this result are repeated flashes of white light from a xenon arc with very good optical coupling to the sample and a significant interval between flashes to avoid accumulated temperature rise in the sample. The efficacy of the flashes of white light of high intensity may be due to the existence of optical transitions extending well into the near-infrared region and possibly as far as suggested by the theoretical studies of Waleh & Loew (1982).

Under such conditions, we reiterate that the X-ray absorption data are best fitted (see Table I) by a single photoproduct, and a 15 times worse fit is obtained by various proportions of MbCO and Mb. As a further control, a sample intentionally partly photolyzed (three flashes only) was best fitted by the sum of Mb*CO and MbCO, confirming that the X-ray data analysis also can detect incomplete photolysis. It

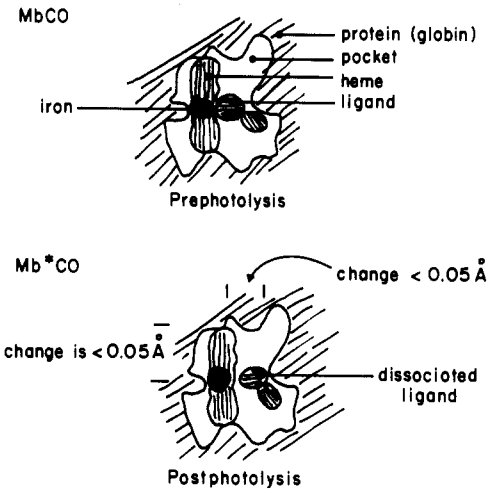

FIGURE 14: Schematic diagram of effect of photolysis on MbCO at 4 K.

appears therefore that completion of photolysis within the accuracy of X-ray data analysis has been achieved.

Structure–Function Relationships. The EXAFS data show that the Mb*CO structure differs from the Mb, which may react directly to form MbCO or which may relax from Mb prior to the reaction with CO, and both steps may involve a tunneling process (Frauenfelder, 1979; Chance et al., 1979). Our symbolic representation of the geminate state (Mb*CO) indicates that CO is still present near the active site, and this geometry change together with Fe–N_p expansion on photolysis are indicated in Figure 14. In addition to our emphasis on distance changes, photolysis may have also altered the geometry of the CO molecule. The possibility of rotation of the CO molecule from its preferred orientation has occurred as suggested by Hush from studies of the octapole moment of model CO compounds (Grady et al., 1978) and in the case of Mb*CO by Alben et al. (1980). In fact, the CO molecule may have tumbled so that the oxygen atom is presented to iron, or the angle of the CO with respect to the heme plane does not provide sufficient overlap for bonding. In that case, motion of the CO back to the initial position would be a step of low activation energy (Austin et al., 1975), as appears to be consistent with the more recent work of Alben et al. (1981). However, such a change in configuration of the CO molecule would be expected to alter the charge density on the heme as reflected in the observed Fe–N_p expansion and associated edge shift, and a change of bond angle remains a preferred hypothesis.

Current studies of elementary steps in biochemical reactions have been based upon geminate states of recently photolyzed MbCO. Obviously, other ligands are of considerable interest and appear to be feasible for further structural studies. In such cases, trapped states indicating the motion of the ligand toward the metal atom in recombination processes are expected to be of great interest in elucidating the nature of elementary steps in chemical reactions and in tunneling processes.

Acknowledgments

It is a pleasure to acknowledge the help of several colleagues in data gathering and sample preparation, especially Y. Ching, B. Muhoberac, and R. Korszun.

References

Alben, J. O., Beece, D., Bowne, S. F., Eisenstein, L., Frauenfelder, H., Good, D., Marden, M. C., Moh, P. P., Reinisch, L., Reynolds, A. H., & Yue, K. T. (1980) *Phys. Rev. Lett. 44*, 1157–1160.

Alben, J. O., Fiamingo, F. G., & Altschuld, R. A. (1981) VIIth International Biophysics Congress and IIIrd Pan-Am Biochemical Congress, Mexico City, Mexico, p 64, M-C12.

Alben, J. O., Beece, D., Bowne, S. F., Doster, W., Eisenstein, L., Frauenfelder, H., Good, D., McDonald, J. C., Marden, M. C., Moh, P. P., Reinisch, L., Reynolds, A. G., & Yue, K. T. (1982) *Proc. Natl. Acad. Sci. U.S.A. 79*, 3744–3748.

Alberding, N., Austin, R., Beeson, K., Chan, S., Eisenstein, L., Frauenfelder, H., & Nordlund, T. (1976a) *Science (Washington, D.C.) 192*, 1002–1003.

Alberding, N., Austin, R. H., Chan, S. S., Eisenstein, L., Frauenfelder, H., Gunsalus, I. C., & Nordlund, T. M. (1976b) *J. Chem. Phys. 65*, 4701–4711.

Alberding, N., Chan, S., Eisenstein, L., Frauenfelder, H., Good, D., Gunsalus, I. C., Nordlund, T. M., Perutz, M. F., Reynolds, A. H., & Sorensen, L. B. (1978) *Biochemistry 17*, 43.

Austin, R. H., Beeson, K. W., Eisenstein, L., Frauenfelder, H., Gunsalus, I. C., & Marshall, V. P. (1973) *Science (Washington, D.C.) 181*, 541–543.

Austin, R. H., Beeson, K. W., Eisenstein, L., Fauenfelder, H., & Gunsalus, I. C. (1975) *Biochemistry 14*, 5355–5373.

Azaroff, L. (1963) *Rev. Mod. Phys. 35*, 1012–1022.

Belli, M., Scafati, A., Bianoconi, A., Mobilio, S., Palladino, L., Reale, A., & Burattini, E. (1980) *Solid State Commun. 35*, 355.

Bücher, H. (1947) *Biochim. Biophys. Acta 1*, 21–34.

Chance, B. (1953) *J. Biol. Chem. 202*, 407–416.

Chance, B., & Powers, L. (1981a) VIIIth Annual Stanford Radiation Laboratory Users Group Meeting, Oct 19 and 20, Stanford, CA.

Chance, B., & Powers, L. (1981b) VIIth International Biophysics Congress and IIIrd Pan-Am Biochemical Congress, Mexico City, Mexico, p 65, M-C14.

Chance, B., Smith, L., & Castor, L. (1953) *Biochim. Biophys. Acta 12*, 289–298.

Chance, B., Schoener, B., & Yonetani, T. (1965) in *Oxidases and Related Redox Systems, Proceedings of a Symposium* (King, T. E., Mason, H. S., Morrison, M., Eds.) p 609, Wiley, New York.

Chance, B., Graham, N., & Legallais, V. (1975) *Anal. Biochem. 67*, 552–579.

Chance, B., Saronio, C., Leigh, J. S., Jr., & Waring, A. (1979) in *Tunneling in Biological Systems* (Chance, B., DeVault, D., Frauenfelder, H., Marcus, R., Schrieffer, J., & Sutin, N., Eds.) pp 483–496, Academic Press, New York.

Chance, B., Fischetti, R., D'Ambrosio, C., Angiolillo, P., Yonetani, T., Powers, L., Perutz, M., & Frauenfelder, H. (1980a) Stanford Synchrotron Radiation Laboratory Activity Report 80/01.

Chance, B., Angiolillo, P., Yang, E., & Powers, L. (1980b) *FEBS Lett. 112*, 178–182.

Chance, B., Pennie, W., Carman, M., Legallais, V., & Powers, L. (1982a) *Anal. Biochem. 124*, 248–257.

Chance, B., Fischetti, R., Sivaram, A., & Powers, L. (1982b) *Biophys. J. 37*, 368a.

Chance, B., Moore, J., Powers, L., & Ching, Y. (1982c) *Anal. Biochem. 124*, 239–247.

Chin, H. B., & Bau, R. (1976) *J. Am. Chem. Soc. 98*, 2434.

Collins, D., Countryman, R., & Hoard, J. L. (1972) *J. Am. Chem. Soc. 94*, 2066–2073.

Cornelius, P. A., Steele, A. W., Chernoff, D. A., & Hochstrasser, R. M. (1981) *Proc. Natl. Acad. Sci. U.S.A. 78*, 7526–7529.

Eisenberger, P., & Lengler, B. (1980) *Phys. Rev.* [*Sect.*] *B 22*, 3551–3562.

Eisenberger, P. M., Shulman, R. G., Kinchaid, B. M., Brown, G. S., & Ogawa, S. (1978) *Nature (London) 274*, 30–34.
Figgis, B. N., Gerloch, M., & Mason, R. (1969) *Proc. R. Soc. London, Ser. A 309*, 91–118.
Fischetti, R., Sivaram, A., & Chance, B. (1981) VIIth International Biophysics Congress and IIIrd Pan-Am Biochemical Congress, Mexico City, Mexico, p 322, F-M42.
Frauenfelder, H. (1979) in *Tunneling in Biological Systems* (Chance, B., DeVault, D. C., Frauenfelder, H., Marcus, R. A., Schrieffer, J. R., & Sutin, N., Eds.) pp 627–649, Academic Press, New York.
Friedman, J. M., Stepnoski, R. A., Stavola, M., Ondiras, M. R., & Cone, R. L. (1982a) *Biochemistry 21*, 2022–2027.
Friedman, J. M., Rousseau, D. L., Ondiras, M. R., & Stepnoski, R. A. (1982b) *Science (Washington, D.C.) 218*, 1244–1246.
Friedman, J. M., Rousseau, D. L., & Ondiras, M. R. (1982c) *Annu. Rev. Phys. Chem. 37*, 471–491.
Gibson, Q. H. (1959) *Biochem. J. 71*, 293–303.
Grady, J. E., Bacskay, G. B., & Hush, N. S. (1978) *J. Chem. Soc., Faraday Trans. 2 74*, 1430–1440.
Hasinoff, B. B. (1981) *J. Phys. Chem. 85*, 526–531.
Henry, E. R., Sommer, J. H., Hofrichter, J., & Eaton, W. A. (1983) *J. Mol. Biol. 166*, 443–451.
Iizuka, T., Yamamoto, H., Kotani, M., & Yonetani, T. (1974) *Biochim. Biophys. Acta 371*, 126–139.
Keilin, D. (1966) *The History of Cell Respiration and Cytochrome*, Cambridge University Press, Cambridge, England.
Korszun, Z. R., & Moffit, K. (1982) *Biophys. J. 37*, 368a.
Labhardt, A., & Yuen, C. (1979) *Nature (London) 277*, 150–151.
Lee, P. A., Citrin, P. H., Eisenberger, P., & Kincaid, B. M. (1981) *Rev. Mod. Phys. 53*, 769–806.
Marcolin, H. E., Reschke, R., & Trautwein, A. (1979) *Eur. J. Biochem. 96*, 119–123.
Peisach, J., Powers, L., Blumberg, W. E., & Chance, B. (1982) *Biophys. J. 38*, 277–285.
Perutz, M. F., Samar Hasnain, S., Duke, P. J., Sessler, J. L., & Hahn, J. E. (1983) *Nature (London) 295*, 535–538.
Powers, L., Blumberg, W. E., Chance, B., Barlow, C., Leigh, J. S., Jr., Smith, J., Yonetani, T., Vik, S., & Peisach, J. (1979) *Biochim. Biophys. Acta 546*, 520–538.
Powers, L., Chance, B., Ching, Y., & Angiolillo, P. (1981) *Biophys. J. 34*, 465–498.
Powers, L., Ching, Y., Chance, B., & Muhoberac, B. (1982) *Biophys. J. 37*, 403a.
Sessler, J. (1982) Ph.D. Thesis, Stanford University, Stanford, CA.
Spartalian, K., Lang, G., & Yonetani, Y. (1976) *Biochim. Biophys. Acta 428*, 281–290.
Stern, E. A. (1974) *Phys. Rev.* [*Sect.*] *B 10*, 3027–3037.
Takano, T. (1977) *J. Mol. Biol. 110*, 569–584.
Teller, R. G., Finke, R. G., Collman, J. P., Chin, H. B., & Beau, R. (1977) *J. Am. Chem. Soc. 99*, 1104.
Waleh, A., & Loew, G. H. (1982) *J. Am. Chem. Soc. 104*, 2346–2351.
Warburg, O. (1948) *Wasserstoffubertragende*, Deutsche Zertaldruckerei, Berlin.
Yonetani, T., Iizuka, T., Yamamoto, H., & Chance, B. (1973) in *Oxidases and Related Redox Systems, Proceedings of the International Symposium, 2nd* (King, T. E., Mason, H. S., & Morrison, M., Eds.) Vol. I, pp 401–405, University Park Press, Baltimore, MD.

Energy-Transfer Measurements on a Double Fluorescent Labeled Ribonuclease A†

Magali Jullien* and Jean-Renaud Garel

ABSTRACT: Two fluorescent groups have been covalently attached to ribonuclease A: first, the α-amino group is labeled upon reaction with fluorescein isothiocyanate, and second, one of the active site histidine residues is modified by *N*-[[(iodoacetyl)amino]ethyl]-5-naphthylamine-1-sulfonic acid. Among the products of these two successive chemical modifications, a derivative bearing one label on Lys-1 and the other label on His-119 can be isolated and characterized. Because of their spectral properties, these two fluorophores, fluorescein and *N*-[(acetamido)ethyl]-5-naphthylamine-1-sulfonic acid, are suitable for measuring resonance energy transfer within a single protein molecule. The efficiency of the energy transfer is close to 100% in the native state and is reduced to about 50% in the guanidine-unfolded state. This efficiency is further diminished upon reduction of the disulfide bonds in denaturing conditions. The efficiency of energy transfer has been determined independently from both emission and excitation spectra of the double-labeled protein, when unfolded with intact disulfide bonds. The average distance between the two fluorescent groups can be obtained from these measurements: it increases from 20 Å at most in the native state to 46 Å or more in the unfolded state.

The intrinsic sensitivity of fluorescence measurements and the variety of reagents available have increased the use of fluorescent labels as conformational probes of biological structures. Nonradiative energy transfer between a suitable donor–acceptor pair can occur provided that the emission spectrum of the donor overlaps the excitation spectrum of the acceptor and that the distance and relative orientation of the two fluorescent groups be appropriate (Stryer, 1978). This energy transfer can be used to measure the distance between the donor and acceptor: depending on the donor–acceptor pair, distances ranging from 10 to 100 Å can be estimated (Fairclough & Cantor, 1978). In many cases, changes in the distance between donor and acceptor, rather than the distance itself, have been measured, especially for complex formation

† From the Unité de Biochimie Cellulaire, Département de Biochimie et Génétique Moléculaire, Institut Pasteur, 75724 Paris Cedex 15, France. *Received December 14, 1982.* This work was supported by the Centre National de la Recherche Scientifique (G.R. No. 30) and the Institut Pasteur.

0006-2960/83/0422-3829$01.50/0